LETTERS
https://doi.org/10.1038/s41591-018-0117-4
nature medicine

Cytotoxic CD8+ T cells recognize and kill *Plasmodium vivax*–infected reticulocytes

Caroline Junqueira[1,2,3]*, Camila R. R. Barbosa[1], Pedro A. C. Costa[1], Andréa Teixeira-Carvalho[1], Guilherme Castro[1], Sumit Sen Santara[2,3], Rafael P. Barbosa[2,3], Farokh Dotiwala[2,3], Dhelio B. Pereira[4], Lis R. Antonelli[1], Judy Lieberman[2,3]* and Ricardo T. Gazzinelli[5,6,7]*

Plasmodium vivax **causes approximately 100 million clinical malaria cases yearly[1,2]. The basis of protective immunity is poorly understood and thought to be mediated by antibodies[3,4]. Cytotoxic CD8+ T cells protect against other intracellular parasites by detecting parasite peptides presented by human leukocyte antigen class I on host cells. Cytotoxic CD8+ T cells kill parasite-infected mammalian cells and intracellular parasites by releasing their cytotoxic granules[5,6]. Perforin delivers the antimicrobial peptide granulysin and death-inducing granzymes into the host cell, and granulysin then delivers granzymes into the parasite. Cytotoxic CD8+ T cells were thought to have no role against *Plasmodium* spp. blood stages because red blood cells generally do not express human leukocyte antigen class I[7]. However, *P. vivax* infects reticulocytes that retain the protein translation machinery. Here we show that *P. vivax*–infected reticulocytes express human leukocyte antigen class I. Infected patient circulating CD8+ T cells highly express cytotoxic proteins and recognize and form immunological synapses with *P. vivax*–infected reticulocytes in a human leukocyte antigen–dependent manner, releasing their cytotoxic granules to kill both host cell and intracellular parasite, preventing reinvasion. *P. vivax*–infected reticulocytes and parasite killing is perforin independent, but depends on granulysin, which generally efficiently forms pores only in microbial membranes[8]. We find that *P. vivax* depletes cholesterol from the *P. vivax*–infected reticulocyte cell membrane, rendering it granulysin-susceptible. This unexpected T cell defense might be mobilized to improve *P. vivax* vaccine efficacy.**

Although less virulent than *Plasmodium falciparum*, *P. vivax* can cause life-threatening cerebral malaria, acute respiratory distress syndrome, splenic rupture, hepatitis, severe anemia and thrombocytopenia, and aggravate comorbidities[9–11]. Both CD8+ T cell interferon-γ (IFN-γ) and cytotoxicity protect against the *Plasmodium* circumsporozoite stages in hepatocytes[12–15], but cytotoxic CD8+ T cells (CTLs) have no known role in fighting the blood stage, which is responsible for clinical pathology. Because host cell invasion requires merozoite Duffy Binding Protein (DBP) interaction with reticulocyte (Retic) Duffy Protein (DP)[16], inducing anti-DBP blocking antibodies is currently the main strategy for an anti–*P. vivax* malaria vaccine[17]. However, anti-DBP vaccines have not been successful in preclinical models, and new vaccine approaches are badly needed[3,4].

Although CD8+ T cells were not expected to recognize the blood-stage parasite, we analyzed activation markers on circulating CD8+CD3+ T cells from uncomplicated *P. vivax* malaria patients by flow cytometry (Fig. 1a,b). These cells were primarily conventional T cell antigen receptor αβ (TCRαβ) CD8+ T lymphocytes (Supplementary Fig. 1a,b). Although the abundance of circulating CD8+ T cells and other lymphocytes (natural killer (NK), γδ T cells, natural killer T (NKT) cells) that might contribute to malaria immune defense did not differ in patients and healthy donors (HDs) from the same endemic region of Brazil (Supplementary Fig. 1c,d), CD8+ T cells from untreated patients had increased expression of CD69 and human leukocyte antigen D–related (HLA-DR) activation markers and Ki67, a cell proliferation indicator. These markers returned to levels similar to those in HDs 30–40 days after treatment with chloroquine and primaquine and parasitological cure. Circulating CD8+ T cell expression of cytotoxic granule granzyme B (GzmB), perforin (PFN) and granulysin (GNLY) was also considerably increased in malaria patients compared with HDs from the endemic area (Fig. 1c,d). These results confirm studies suggesting that circulating CD8+ T cells are activated during *P. vivax*, and to a lesser extent *P. falciparum*, infection[18–22]. Acute patient plasma also contained ~6-fold more GNLY than HD plasma by ELISA (Fig. 1e). To identify the source of GNLY, we analyzed innate, innate-like and conventional αβ T cells from HDs and acute malaria patients for GNLY expression (Supplementary Fig. 1e). Most GNLY+ circulating lymphocytes in patients were conventional CD8+ T cells (69.7% ± 1.2%). A higher proportion of GNLY+ circulating lymphocytes were conventional CD8+ T cells in patients than HDs ($P = 0.03$). Fewer than 10% of the circulating GNLY+ cells were CD4+ T cells, γδ T cells, NK cells, or NKT cells in either patients or HDs. Thus, conventional CD8+ T cells express most of the GNLY in infected patients.

On the basis of these data, we hypothesized that CD8+ T cells in patients with *P. vivax* malaria might become activated by recognizing *P. vivax*–infected reticulocytes (iRetics), causing them to degranulate and release GNLY. Although *P. falciparum* infects mature red blood cells (RBCs), asexual *P. vivax* exclusively infects Retics, which retain the translation machinery, endoplasmic reticulum and Golgi apparatus needed to produce cell surface proteins. An early electron microscopy study suggested that human Retics weakly express human leukocyte antigen class I (HLA-I)[7]. More recent transcriptome and proteome analyses indicated that Retics express HLA and

[1]Instituto René Rachou, Fundação Oswaldo Cruz, Belo Horizonte, Brazil. [2]Program in Cellular and Molecular Medicine, Boston Children's Hospital, Boston, MA, USA. [3]Department of Pediatrics, Harvard Medical School, Boston, MA, USA. [4]Centro de Pesquisas em Medicina Tropical, Porto Velho, Brazil. [5]Plataforma de Medicina Translacional, Fundação Oswaldo Cruz, Ribeirão Preto, Brazil. [6]Departamento de Bioquímica e Imunologia, Universidade Federal de Minas Gerais, Belo Horizonte, Brazil. [7]Division of Infectious Disease and Immunology, University of Massachusetts Medical School, Worcester, MA, USA. *e-mail: carolinejunqueira@minas.fiocruz.br; judy.lieberman@childrens.harvard.edu; ricardo.gazzinelli@umassmed.edu

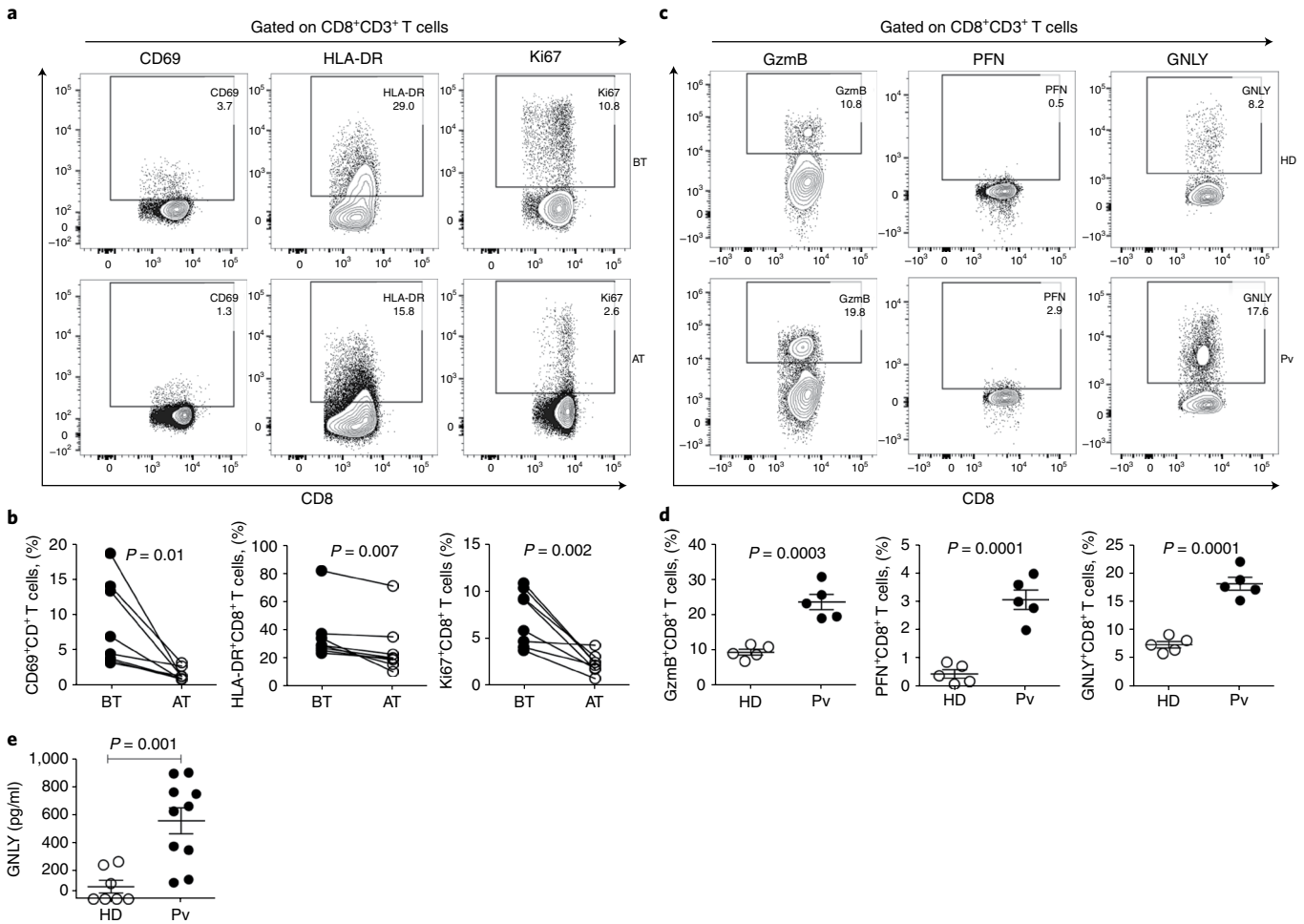

Fig. 1 | Increased frequency of activated CD8⁺ T cells in the peripheral blood of *P. vivax* patients. PBMCs from HDs and *P. vivax* malaria patients (Pv) were gated on CD8⁺CD3⁺ T cells (gating strategy described in Supplementary Fig. S1) and analyzed for expression of activation markers and cytotoxic granule proteins by flow cytometry. **a**,**b**, Shown are representative flow plots (**a**) and the proportion of malaria patients' CD8⁺ T cells expressing CD69, HLA-DR and Ki67 (**b**) before treatment (BT) and 30–40 days after treatment and parasitological cure (AT). $n = 8$ biologically independent samples/independent experiments. Statistical analysis was performed by two-tailed parametric paired *t*-test at 95% CI. **c**,**d**, Shown are representative flow plots (**c**) and the proportion of HD and Pv peripheral blood CD8⁺ T cells expressing GzmB, PFN, and GNLY (**d**) BT. $n = 5$ biologically independent samples/independent experiments. **e**, The levels of soluble GNLY in plasma of $n = 7$ HD and $n = 10$ Pv BT were measured by ELISA as biologically independent samples/independent experiments. In **d**,**e**, mean ± s.e.m. is shown; statistical analysis was performed by two-tailed nonparametric unpaired *t*-test at 95% CI.

proteins involved in antigen presentation[23,24], including the proteasome, TAP transporter and cofactor TAPASIN, and the endoplasmic reticulum aminopeptidase ERAP1 (Supplementary Table S1). We therefore used a pan⁻ class I antibody to compare HLA-I expression on the surface of uninfected and iRetics from patients and HDs. iRetics were identified by SYBR Green I staining[25], which stains parasite DNA, but not Retic RNA (Supplementary Fig. 2). RBCs were gated based on size and granularity and CD235a (glycophorin A) staining (Fig. 2a), and Retics were identified as CD235a⁺ and CD71⁺ (transferrin receptor). As expected[26], acute malaria patient

Fig. 2 | Increased HLA-ABC in *P. vivax*–infected reticulocytes. a, Gating strategy to evaluate *P. vivax* infection and HLA expression in reticulocytes. Top and bottom panels are representative results from an HD and patient with *P. vivax* acute malaria (Pv) before treatment (BT), respectively. Retics are CD71⁺CD235a⁺, and SYBR Green detects parasite DNA in iRetics. A pan-HLA class I antibody was used to analyze HLA expression. This experiment was repeated four times with similar results. **b**–**d**, Comparison of percent of retics in the RBC gate (**b**), percent of Retics that express HLA-I (**c**), and percent of SYBR Green⁺ iRetics (**d**) in blood from HDs ($n = 8$) and Pv BT patients ($n = 8$). Shown are mean ± s.e.m.; statistical analysis by two-tailed nonparametric unpaired *t*-test at 95% CI. **e**, Comparison of HLA-ABC expression in circulating uRetics and iRetics in $n = 8$ Pv BT samples, based on SYBR Green I and HLA staining of CD235a⁺CD71⁺ Retics, representative dot plot in **a**. Shown are mean ± s.e.m.; statistical analysis used a two-tailed parametric paired *t*-test at 95% CI. **f**,**g**, Comparison of HLA-ABC (**f**) and HLA-DR (**g**) expression by HD uRetics and Pv iRetics and CD19⁺ B cells. Light gray histograms are unstained, and darker gray histograms are stained cells. Shown are representative samples of five analyzed. **h**, Imaging flow cytometry of representative Pv uRetics (top) and iRetics (bottom) stained for CD235a, SYBR Green, CD71, HLA-ABC and HLA-DR. This experiment was repeated three times with similar results. **i**, Immunoblot of cell lysates from three HD uRetics and three Pv iRetics, loaded with 50 μg of protein/well and probed for the antigen processing protein, TAP1, as well as β-actin and F-actin as loading controls for HD uRetics and Pv BT iRetics, respectively. HD PBMCs were used as a positive control (20 μg). This experiment was repeated three times with similar results.

RBCs contained ~5-fold more Retics than HDs (Fig. 2b). About half of patient Retics stained for HLA-I, compared with ~10% in HDs ($P < 0.0001$) (Fig. 2c). Of circulating Retics from patients, 50.3% ± 7.0% were infected (Fig. 2d), and 57.1% ± 7.9% of iRetics expressed HLA-I at levels comparable with that on B lymphocytes (Fig. 2e,f) but did not express HLA-DR (Fig. 2g). In contrast, <20% of uninfected SYBR Green$^-$ Retics from patients expressed HLA-I ($P < 0.0001$). Imaging flow cytometry confirmed HLA-I expression selectively on iRetics, compared with HD Retics (Fig. 2h).

Cell surface HLA expression depends on antigenic peptide binding[27]. To confirm that iRetics have the antigen processing machinery, we used density separation to isolate iRetics from

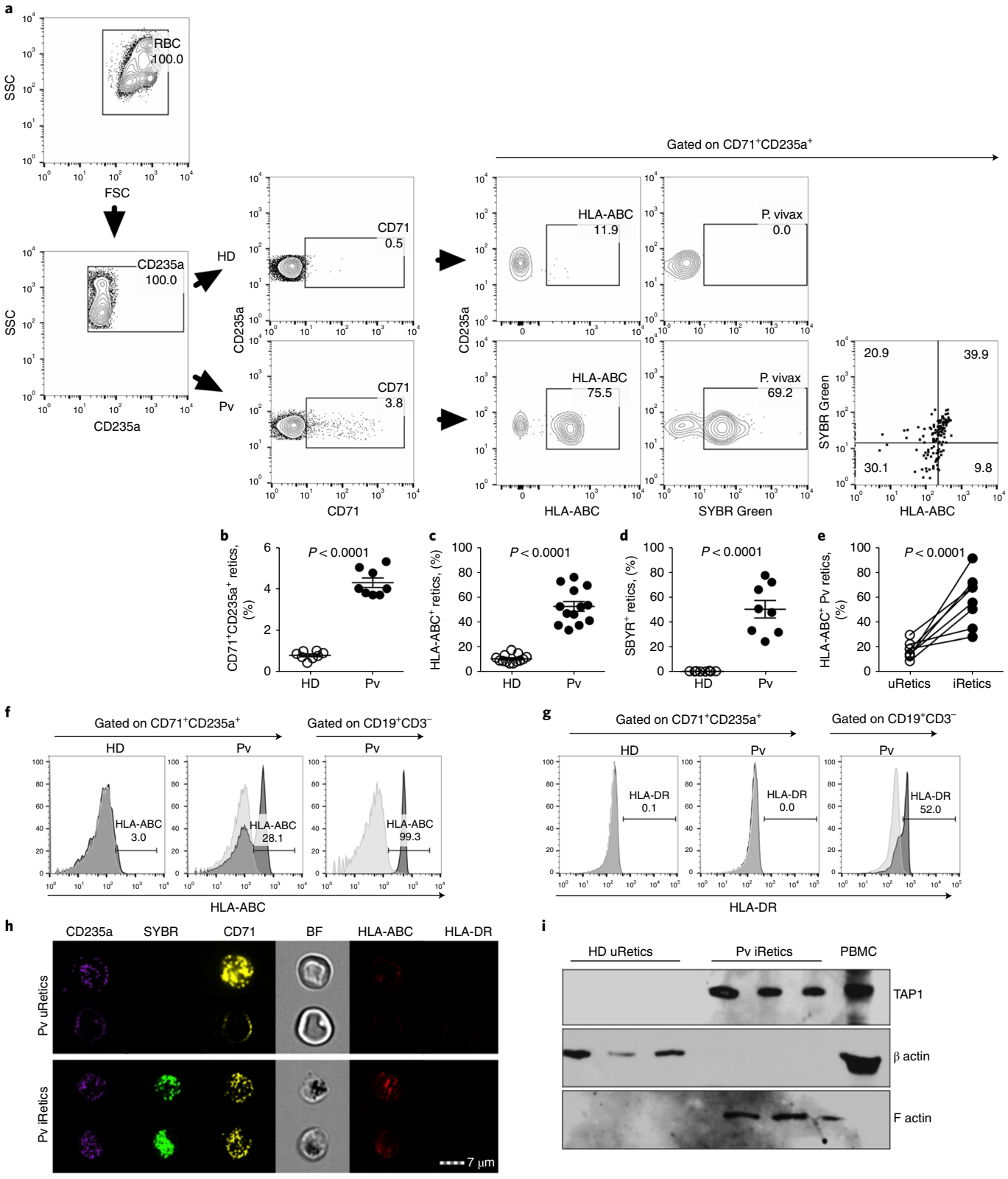

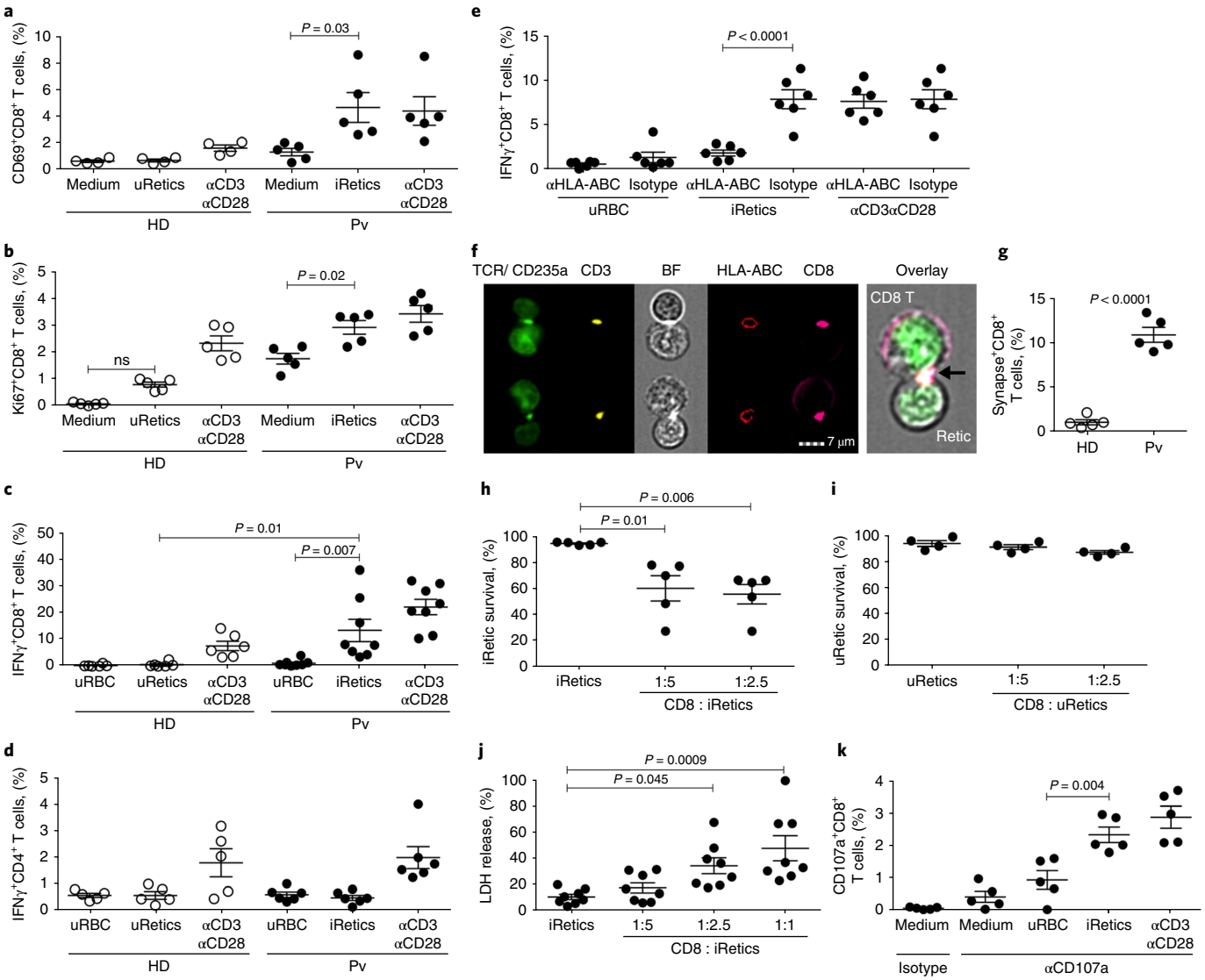

Fig. 3 | CD8⁺ T cells are activated by and lyse autologous *P. vivax*-infected reticulocytes. a–d, Purified CD8⁺ or CD4⁺ T lymphocytes from HDs or patients with *P. vivax* malaria (Pv) before treatment (BT) were cultured in medium alone, with autologous uRetics, with purified iRetics, or in the presence of anti-CD3 and anti-CD28, and analyzed by flow cytometry for the proportion of CD8⁺ T cells staining for CD69 (**a**) and Ki67 (**b**) ($n=5$) or intracellular IFN-γ (**c**) ($n=8$), or CD4⁺ T cells staining for intracellular IFN-γ (**d**) ($n=6$). **e**, IFN-γ expression by CD8⁺ T cells after stimulation with autologous uninfected RBCs (uRBC), purified iRetics, or anti-CD3 and anti-CD28 in the presence of anti-HLA-ABC or isotype control antibody ($n=6$). **f**,**g**, Imaging flow cytometry analysis of immune synapse formation between CD8⁺ T cells and autologous purified iRetics from Pv or uRetics from HDs ($n=5$). Shown are representative images of immunological synapses between CD8⁺ T cells and purified iRetics from a Pv sample, arrow indicates immunological synapse, i.e., overlay staining of anti-TCR, anti-CD3, anti-HLA-ABC and anti-CD8 labeled antibodies (**f**) and mean ± s.e.m. of the proportion of CD8⁺ T cells forming synapses in five HD samples with autologous uRetics and in five Pv BT samples with purified iRetics (**g**). $n=5$ biologically independent samples/independent experiments. Cells were stained for TCR and CD235a, CD3, HLA-ABC, and CD8, and synapses were identified by the capping and colocalization of TCR, CD3, CD8, and HLA-ABC where the T cell and RBC are juxtaposed. The enlarged overlay image on the right corresponds to the bottom image. **h**,**i**, Survival of iRetics after 12-h incubation with medium or autologous CD8⁺ T cells from Pv samples ($n=5$) (**h**) or of uRetics incubated with medium or autologous HD CD8⁺ T cells ($n=4$) (**i**), added at indicated E:T ratios, as assayed using CFSE-labeled Retics. **j**, iRetic lysis after 12-h incubation with medium or autologous CD8⁺ T cells from Pv samples ($n=8$), measured by LDH release. **k**, Frequency of CD8⁺ T cells in the blood of five untreated Pv that degranulate, assessed by CD107a staining, in response to indicated stimuli. Shown are mean ± s.e.m.; statistical analysis by nonparametric two-way ANOVA (**a**–**e**), two-tailed nonparametric unpaired *t*-test at 95% CI (**g**), and nonparametric one-way ANOVA (**h**–**k**).

three infected donors and uninfected Retics (uRetics) from three HDs (Supplementary Fig. 3a,b), and analyzed their expression of TAP1 by immunoblot. TAP1 was readily detected in iRetics, but not uRetics (Fig. 2i). Thus, iRetics selectively express HLA-I and TAP1, suggesting they might present malaria antigens to CD8⁺ T cells.

Long-term *P. vivax* culture has not been possible, limiting studies of the immune response to blood-stage infection. We developed a short-term in vitro culture system[19,28,29] that enabled us to study the CD8⁺ T cell response to iRetics. CD8⁺ T cells, isolated by immunomagnetic selection from HDs or patients, were cultured for 10 h with autologous, enriched uRetics or iRetics, respectively (Supplementary Fig. 3c). iRetic incubation activated infected donor CD8⁺ T cells to express CD69 and Ki67 and produce IFN-γ (Fig. 3a–c). In contrast, HD CD8⁺ T cells did not respond to uRetics.

Both patient and HD $CD8^+$ T cells were activated by anti-CD3/anti-CD28. Neither patient nor HD $CD4^+$ T cells responded to iRetics (Fig. 3d). Importantly, HLA-I blocking, but not control, antibody[30] prevented iRetic-induced IFN-γ production by $CD8^+$ T cells, but did not affect anti-CD3/anti-CD28 activation, which does not require HLA-I (Fig. 3e). Thus, circulating $CD8^+$ T cells in infected patients specifically recognize HLA-I–bound antigens on iRetics.

Imaging flow cytometry was next used to visualize the $CD8^+$ T cell–iRetic interaction, by staining cocultures for HLA-I, CD235a, CD3, CD8 and TCR (Fig. 3f,g). Of circulating $CD8^+$ T cells from five malaria donors, 10.9% ± 2.2% formed immune synapses in which TCR, CD3 and CD8 on the T cell capped and colocalized with HLA-I on autologous iRetics. By contrast, <1% of HD $CD8^+$ T cells formed synapses with autologous Retics. To examine whether $CD8^+$ T cells lyse iRetics, we cocultured carboxyfluorescein diacetate succinimidyl ester (CFSE)–stained infected donor or HD Retics at different ratios with autologous $CD8^+$ T cells, and assessed by flow cytometry the persistence of CFSE-stained cells 12 h later (Fig. 3h,i). Infected donor $CD8^+$ T cells considerably reduced the number of iRetics, but HD $CD8^+$ T cells did not affect uRetics, indicating the specificity of iRetic lysis in infected patients. iRetic lysis by autologous patient $CD8^+$ T cells was confirmed by measuring lactate dehydrogenase (LDH) release that increased with more $CD8^+$ T cells (Fig. 3j). Activated $CD8^+$ T cells kill infected cells by cytotoxic granule exocytosis, which can be measured by externalization of LAMP-1 (CD107a). After incubation with autologous iRetics, but not uninfected RBCs, infected donor $CD8^+$ T cells stained for surface CD107a, indicating that they degranulated (Fig. 3k). Moreover, the numbers of $CD107a^+CD8^+$ T cells after iRetic coculture were not considerably different from the numbers that degranulated after anti-CD3/anti-CD28 treatment, suggesting that most of the circulating activated $CD8^+$ CTLs in infected donors specifically recognize iRetics.

CTLs kill other intracellular parasites in a PFN-, GNLY-, and Gzm-dependent manner[5]. To determine how iRetics are lysed and whether *P. vivax* are killed in the process, we first used imaging flow cytometry to determine whether Alexa Flour 488 (AF488)–labeled GNLY and/or GzmB bound and/or entered uRetics or iRetics (Fig. 4a–f). GNLY, but not GzmB on its own, selectively bound to iRetics, but not uRetics (Fig. 4a–d). Moreover, when GNLY was present, virtually all iRetics, but not uRetics, stained with GzmB (Fig. 4e,f). GNLY colocalized with CD235a on the iRetic membrane, whereas GzmB was internalized and colocalized with intracellular *P. vivax*, stained with a Hoechst DNA dye (Fig. 4g, Supplementary Fig. 4). In some iRetics, GzmB also showed punctate host cell staining, which might represent GzmB trafficking to host mitochondria, where Gzms concentrate[31]. Thus, GNLY, independently of PFN, delivers GzmB to the parasite, a surprising finding, because in other intracellular parasite infections, PFN is required to deliver GNLY and Gzms across host cell membranes[5].

GNLY permeabilizes cholesterol-containing mammalian cell membranes only at exceedingly high (micromolar) concentrations, because cholesterol inhibits pore formation[8]. In contrast, PFN is a cholesterol-dependent cytolysin. Other *Plasmodium* species harvest and deplete cholesterol from RBC membranes[32,33], which could make them susceptible to GNLY. When we depleted cholesterol from RBC membranes using methyl-β-cyclodextrin, AF488-labeled GNLY attached to the cholesterol-depleted, but not to untreated, RBC membranes (Fig. 4h), delivered GzmB–AF488 into the RBCs (Fig. 4i), and lysed cholesterol-depleted RBCs (Fig. 4j). To determine whether cholesterol was depleted from iRetic membranes, we stained Retics with 25-[*N*-[(7-nitro-2-1,3-benzoxadiazol-4-yl)methyl]amino]-27-norcholesterol (25-NBD-cholesterol), a fluorescent cholesterol mimic. iRetics, but not uRetics, stained brightly with 25-NBD-cholesterol (Fig. 4k,l), suggesting that *P. vivax* also harvests cholesterol from iRetic membranes, making them GNLY-susceptible.

GNLY-delivered GzmB colocalization with the parasite (Fig. 4g) suggested that GNLY and GzmB would not only lyse iRetics, but might also directly kill the parasite. To determine which cytotoxic molecules are required to lyse iRetics and whether intracellular parasites are also killed, we incubated GNLY, GzmB, and/or PFN with iRetics (Fig. 4m) or HD uRetics (Fig. 4n) for 1 h and measured RBC lysis by LDH release and parasite viability by the ability to invade fresh Retics[34] (Fig. 4o). GNLY on its own lysed iRetics, but GzmB or PFN, alone or together, had no substantial effect. However, GNLY and GzmB were considerably more cytotoxic than GNLY, and GzmB, GNLY, and PFN further substantially enhanced iRetic lysis. Importantly, uRetics were unaffected by GzmB or GNLY, but were lysed by PFN, as expected, because their membranes are cholesterol rich. GNLY alone inhibited parasite invasion of fresh RBCs, but GNLY and GzmB together or all three cytotoxic molecules completely blocked reinvasion. Reinvasion could be inhibited because of parasite killing or because parasite maturation or infectious merozoite release was hindered. To determine whether the parasites within iRetics were directly damaged, we analyzed iRetic morphology by electron microscopy after treatment with GNLY ± GzmB (Fig. 4o). After just GNLY, the treated iRetics swelled and the intracellular parasites started to show signs of death, such as cytoplasmic vacuolization, consistent with iRetic membrane damage by GNLY. However, after incubation with both GNLY and GzmB, intracellular parasites developed swollen and fragmented mitochondria, condensed nuclei, and cytoplasmic vacuolization, and the parasitophorous vacuole membrane was disrupted (Fig. 4p). These changes resembled morphological changes seen after GzmB and GNLY treatment of other protozoan parasites[5]. The protocol used

Fig. 4 | Granulysin binds to infected reticulocytes and mediates host cell lysis and parasite killing. a–f, Imaging flow cytometry analysis of uptake of GzmB–AF488 (**a**,**b**) or GNLY–AF488 (**c**,**d**) on their own, or of GzmB–AF488 in the presence of unlabeled GNLY (**e**,**f**) by HD uRetics and by uRetics and iRetics from patients with acute untreated *P. vivax* (Pv). In **a**,**c**,**e**, Representative images are shown; In **b**,**d**,**f**, mean ± s.e.m. of three HD and Pv samples are shown. **g**, Imaging flow cytometry images of Pv uRetics and iRetics incubated with GzmB–AF488 and GNLY–AF750, and stained for CD235a and with a Hoechst dye to stain parasite DNA. This experiment was repeated three times with similar results. **h**–**j**, Effect of methyl-β-cyclodextrin depletion of cholesterol in HD RBCs on binding of GNLY–AF488 on its own ($n = 4$) (**h**), binding of GzmB-AF488 in the presence of unlabeled GNLY ($n = 3$) (**i**), and on RBC lysis by increasing amounts of GNLY, assessed by LDH release ($n = 4$) (**j**). Shown are *P* values in comparison to untreated RBCs. **k**,**l**, Staining of HD uRetics and of untreated Pv uRetics and iRetics with the cholesterol analog 25-NBD ($n = 3$). Representative images are shown in (**k**) ($n = 5$), and the proportion of cells with detectable 25-NBD fluorescence is shown in (**l**) ($n = 4$). **m**,**n**, Cytolysis of Pv iRetics (**m**) ($n = 5$) or HD uRetics (**n**) ($n = 4$) after 1-h incubation with GzmB ± GNLY ± PFN, assessed by LDH release. **o**, Effect of incubation of iRetics from four Pv for 1h with indicated cytotoxic granule proteins on parasite invasion of fresh Retics, assessed by Giemsa staining. **p**–**r**, Electron micrographs of iRetics that were untreated or incubated with GNLY ± GzmB. Higher magnification images after treatment with GNLY plus GzmB in **q** show parasitophorous vacuole membrane disruption (black arrows) and chromatin condensation (white arrow) (left); cytoplasmic vacuolization (black arrows) and dense granules (white arrows) (middle); and mitochondrial swelling (white arrow) (right). Higher magnification images of untreated cells (**r**) show intact digestive vacuole (black arrow) (left), parasitophorous vacuole membrane (black arrow), and mitochondrion (white arrow) (right). These experiments were repeated three times with similar results (**p**,**r**). Graphs show mean ± s.e.m.; statistics were analyzed by one-way ANOVA (**b**,**d**,**f**,**j**,**l**–**o**) and by two-tailed nonparametric paired *t*-test at 95% CI (**h**,**i**). BF, bright field.

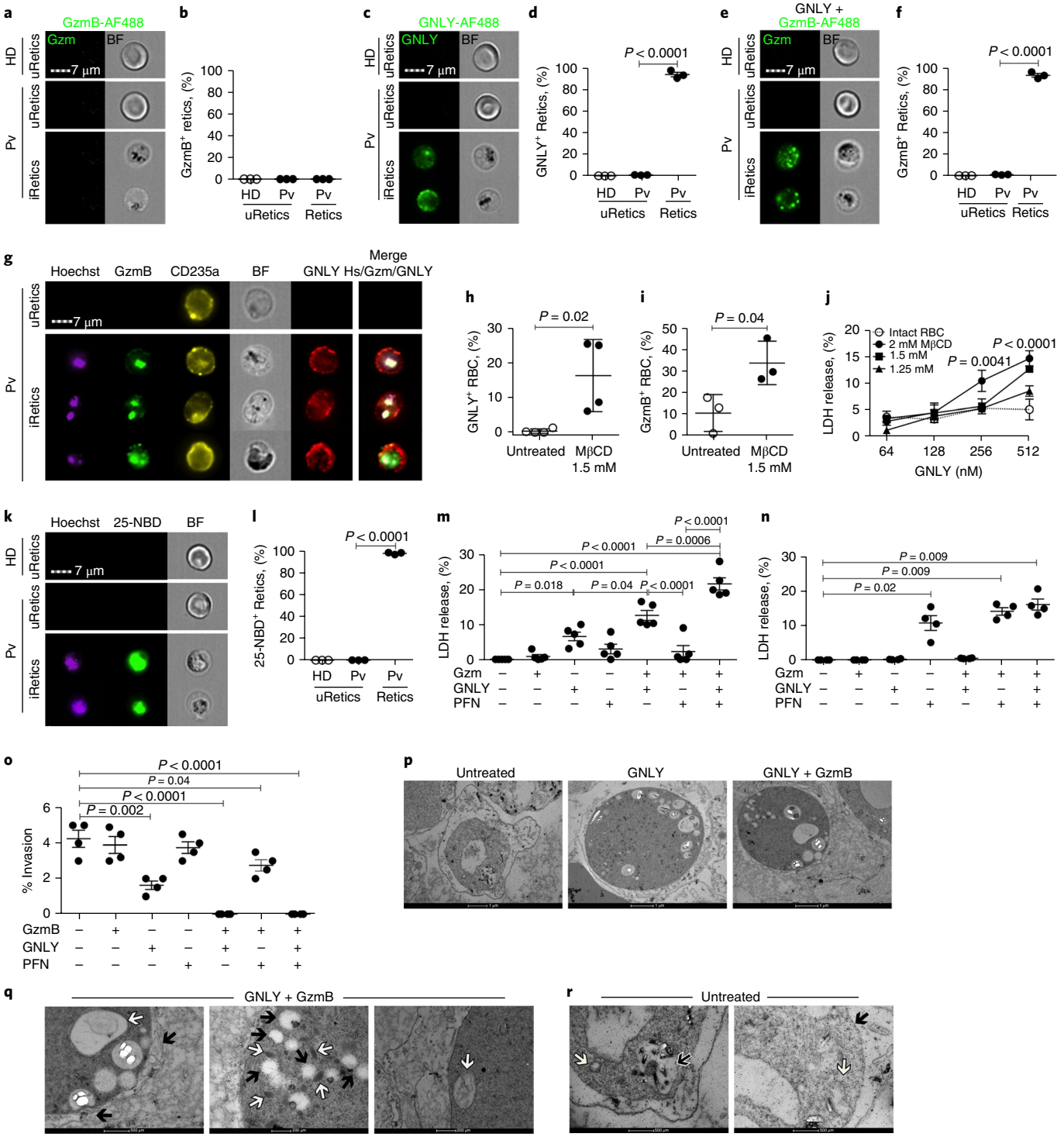

to select iRetics enriches for trophozoite-stage infection. Thus, GNLY and GzmB not only lyse iRetics, but also directly kill intracellular trophozoites and block reinvasion.

In conclusion, *P. vivax* iRetics highly express HLA-I and are specifically recognized by CD8+ T cells. This is, to our knowledge, a unique example of CD8+ T cells recognizing Retics in an HLA-restricted antigen-specific manner. Because GNLY on its own delivers GzmB into iRetics, the CTL mechanism that lyses iRetics is distinct from granule-mediated killing of other mammalian target cells and intracellular parasites, which requires PFN. iRetic lysis would be expected to reduce parasite infectivity by releasing parasites that have not yet matured to the infectious merozoite stage from their obligate intracellular niche. However, here we provide evidence that CD8+ T cells also directly kill *P. vivax*, which should enhance immune effectiveness by limiting spreading of infectious organisms. Whereas patient CTLs lysed iRetics in a 12-h assay, parasite killing and inhibition of reinvasion occurred within an hour of adding GNLY and GzmB, suggesting that parasite death is rapid. The molecular mechanism of *P. vivax* killing remains to be defined, which will be challenging without long-term culture systems for *P. vivax*. Nevertheless, our findings identify a previously unsuspected protective mechanism against blood-stage parasites and suggest that a vaccine that elicits CTLs against blood-stage *P. vivax* may help prevent transmission and control disease

severity. In the future, it will be worthwhile to examine whether other innate or innate-like killer lymphocytes that express GNLY, such as NK and γδ T cells, recognize and kill iRetic and play a role in immune protection[35–39]. Future studies are also needed to determine whether killer lymphocytes are always beneficial during blood-stage malaria, because they might contribute to anemia, inflammation or other pathological sequelae of infection.

Methods

Methods, including statements of data availability and any associated accession codes and references, are available at https://doi.org/10.1038/s41591-018-0117-4.

Received: 6 December 2017; Accepted: 5 June 2018;
Published online: 23 July 2018

References

1. Anstey, N. M., Douglas, N. M., Poespoprodjo, J. R. & Price, R. N. *Plasmodium vivax*: clinical spectrum, risk factors and pathogenesis. *Adv. Parasitol.* **80**, 151–201 (2012).
2. Miller, L. H., Ackerman, H. C., Su, X. Z. & Wellems, T. E. Malaria biology and disease pathogenesis: insights for new treatments. *Nat. Med.* **19**, 156–167 (2013).
3. Zimmerman, P. A., Ferreira, M. U., Howes, R. E. & Mercereau-Puijalon, O. Red blood cell polymorphism and susceptibility to *Plasmodium vivax*. *Adv. Parasitol.* **81**, 27–76 (2013).
4. Mueller, I., Shakri, A. R. & Chitnis, C. E. Development of vaccines for *Plasmodium vivax* malaria. *Vaccine* **33**, 7489–7495 (2015).
5. Dotiwala, F. et al. Killer lymphocytes use granulysin, perforin and granzymes to kill intracellular parasites. *Nat. Med.* **22**, 210–216 (2016).
6. Walch, M. et al. Cytotoxic cells kill intracellular bacteria through granulysin-mediated delivery of granzymes. *Cell* **157**, 1309–1323 (2014).
7. Silvestre, D., Kourilsky, F. M., Nicolai, M. G. & Levy, J. P. Presence of HLA antigens on human reticulocytes as demonstrated by electron microscopy. *Nature* **228**, 67–68 (1970).
8. Barman, H. et al. Cholesterol in negatively charged lipid bilayers modulates the effect of the antimicrobial protein granulysin. *J. Membr. Biol.* **212**, 29–39 (2006).
9. Bassat, Q. & Alonso, P. L. Defying malaria: fathoming severe *Plasmodium vivax* disease. *Nat. Med.* **17**, 48–49 (2011).
10. Murray, C. J. et al. Global malaria mortality between 1980 and 2010: a systematic analysis. *Lancet* **379**, 413–431 (2012).
11. Lacerda, M. V. et al. Understanding the clinical spectrum of complicated *Plasmodium vivax* malaria: a systematic review on the contributions of the Brazilian literature. *Malar. J.* **11**, 12 (2012).
12. Chakravarty, S., Baldeviano, G. C., Overstreet, M. G. & Zavala, F. Effector CD8+T lymphocytes against liver stages of *Plasmodium yoelii* do not require gamma interferon for antiparasite activity. *Infect. Immun.* **76**, 3628–3631 (2008).
13. Spencer, A. J. et al. The threshold of protection from liver-stage malaria relies on a fine balance between the number of infected hepatocytes and effector CD8(+) T cells present in the liver. *J. Immunol.* **198**, 2006–2016 (2017).
14. Schofield, L. et al. Gamma interferon, CD8+T cells and antibodies required for immunity to malaria sporozoites. *Nature* **330**, 664–666 (1987).
15. Seguin, M. C. et al. Induction of nitric oxide synthase protects against malaria in mice exposed to irradiated *Plasmodium berghei* infected mosquitoes: involvement of interferon gamma and CD8+T cells. *J. Exp. Med.* **180**, 353–358 (1994).
16. Miller, L. H., Mason, S. J., Dvorak, J. A., McGinniss, M. H. & Rothman, I. K. Erythrocyte receptors for (*Plasmodium knowlesi*) malaria: Duffy blood group determinants. *Science* **189**, 561–563 (1975).
17. King, C. L. et al. Naturally acquired Duffy-binding protein-specific binding inhibitory antibodies confer protection from blood-stage Plasmodium vivax infection. *Proc. Natl. Acad. Sci. USA* **105**, 8363–8368 (2008).
18. Safeukui, I., et al. Malaria induces anemia through CD8+T cell-dependent parasite clearance and erythrocyte removal in the spleen. *MBio* **6**, e02493-14 (2015).
19. Costa, P. A. et al. Induction of inhibitory receptors on T cells during *Plasmodium vivax* malaria impairs cytokine production. *J. Infect. Dis.* **212**, 1999–2010 (2015).
20. Hojo-Souza, N. S. et al. Phenotypic profiling of CD8(+) T cells during *Plasmodium vivax* blood-stage infection. *BMC Infect. Dis.* **15**, 35 (2015).
21. Burel, J. G., Apte, S. H., McCarthy, J. S. & Doolan, D. L. *Plasmodium vivax* but not *Plasmodium falciparum* blood-stage infection in humans is associated with the expansion of a CD8+T cell population with cytotoxic potential. *PLoS Negl. Trop. Dis.* **10**, e0005031 (2016).
22. Falanga, Y. T., et al. High pathogen burden in childhood promotes the development of unconventional innate-like CD8+T cells. *JCI Insight* **2**, e93814 (2017).
23. Wilson, M. C. et al. Comparison of the proteome of adult and cord erythroid cells, and changes in the proteome following reticulocyte maturation. *Mol. Cell. Proteom.* **15**, 1938–1946 (2016).
24. Goh, S. H. et al. The human reticulocyte transcriptome. *Physiol. Genom.* **30**, 172–178 (2007).
25. Malleret, B. et al. A rapid and robust tri-color flow cytometry assay for monitoring malaria parasite development. *Sci. Rep.* **1**, 118 (2011).
26. Hoffmann, J. J. & Pennings, J. M. Pseudo-reticulocytosis as a result of malaria parasites. *Clin. Lab. Haematol.* **21**, 257–260 (1999).
27. Raghavan, M., Del Cid, N., Rizvi, S. M. & Peters, L. R. MHC class I assembly: out and about. *Trends Immunol.* **29**, 436–443 (2008).
28. Antonelli, L. R. et al. The CD14+CD16+ inflammatory monocyte subset displays increased mitochondrial activity and effector function during acute *Plasmodium vivax* malaria. *PLoS Pathog.* **10**, e1004393 (2014).
29. Rocha, B. C. et al. Type I interferon transcriptional signature in neutrophils and low-density granulocytes are associated with tissue damage in malaria. *Cell Rep.* **13**, 2829–2841 (2015).
30. Heemskerk, M. H. et al. Dual HLA class I and class II restricted recognition of alloreactive T lymphocytes mediated by a single T cell receptor complex. *Proc. Natl. Acad. Sci. USA* **98**, 6806–6811 (2001).
31. Martinvalet, D., Dykxhoorn, D. M., Ferrini, R. & Lieberman, J. Granzyme A cleaves a mitochondrial complex I protein to initiate caspase-independent cell death. *Cell* **133**, 681–692 (2008).
32. Lauer, S. et al. Vacuolar uptake of host components, and a role for cholesterol and sphingomyelin in malarial infection. *EMBO J.* **19**, 3556–3564 (2000).
33. Holz, G. G. Jr. Lipids and the malarial parasite. *Bull. World Health Organ.* **55**, 237–248 (1977).
34. Russell, B. et al. A reliable ex vivo invasion assay of human reticulocytes by *Plasmodium vivax*. *Blood* **118**, e74–e81 (2011).
35. Ramsey, J. M. et al. *Plasmodium falciparum* and *P. vivax* gametocyte-specific exoantigens stimulate proliferation of TCR gammadelta+lymphocytes. *J. Parasitol.* **88**, 59–68 (2002).
36. Artavanis-Tsakonas, K. & Riley, E. M. Innate immune response to malaria: rapid induction of IFN-gamma from human NK cells by live Plasmodium falciparum-infected erythrocytes. *J. Immunol.* **169**, 2956–2963 (2002).
37. Artavanis-Tsakonas, K. et al. Activation of a subset of human NK cells upon contact with *Plasmodium falciparum*-infected erythrocytes. *J. Immunol.* **171**, 5396–5405 (2003).
38. Costa, G. et al. Control of *Plasmodium falciparum* erythrocytic cycle: γδ T cells target the red blood cell-invasive merozoites. *Blood* **118**, 6952–6962 (2011).
39. Troye-Blomberg, M. et al. Human gamma delta T cells that inhibit the in vitro growth of the asexual blood stages of the *Plasmodium falciparum* parasite express cytolytic and proinflammatory molecules. *Scand. J. Immunol.* **50**, 642–650 (1999).

Acknowledgements

We thank Dr. Kasturi Haldar and Kenneth Rock for scientific discussions and suggestions during the development of this work. We are grateful to the Program for Technological Development in Tools for Health–PDTIS-FIOCRUZ for use of its facilities, and to the clinic, laboratory and administrative staff, as well as field workers and subjects from Porto Velho who participated in the study. This study was funded by the National Institutes of Health (1R01NS098747 to R.T.G.; the Amazonian-ICEMR U19 AI089681 to C.J., L.R.A., and R.T.G.; 1R01AI116577 and R21AI131632-01 to R.T.G. and J.L.); National Institute of Science and Technology for Vaccines/Conselho Nacional de Desenvolvimento Científico e Tecnológico (465293/2014-0 to C.J., L.R.A., D.B.P. and R.T.G.) and Fundação de Amparo à Pesquisa do Estado de Minas Gerais (RED-00012-14 and APQ-00653-16 to C.J. and R.T.G.); and Fundação de Amparo à Pesquisa do Estado de São Paulo (2016/23618-8 to R.T.G.). C.J., L.R.A., A.T.-C., and R.T.G. are recipients of CNPq fellowships; P.A.C.C. and C.R.R.B. are fellows from FAPEMIG; and C.J. is a fellow from Coordenação de Aperfeiçoamento de Pessoal de Ensino Superior.

Author contributions

C.J., J.L., and R.T.G. conceived the study. C.J. and R.T.G. supervised this study. D.B.P. recruited the patients and healthy donors; C.J., L.R.A., A.T.-C., J.L., and R.T.G. designed and analyzed experiments. C.J., C.R.R.B., L.R.A., P.A.C.C., A.T.-C., G.C., and R.P.B. performed experiments. S.S.S. and F.D. contributed reagents. C.J., C.R.R.B., P.A.C.C., and L.R.A. prepared figures and helped with manuscript preparation. C.J., J.L., and R.T.G. wrote the paper.

Competing interests

The authors declare no competing interests.

Additional information

Supplementary information is available for this paper at https://doi.org/10.1038/s41591-018-0117-4.

Reprints and permissions information is available at www.nature.com/reprints.

Correspondence and requests for materials should be addressed to C.J. or J.L. or R.T.G.

Publisher's note: Springer Nature remains neutral with regard to jurisdictional claims in published maps and institutional affiliations.

Methods

Malaria patients and healthy donors. Male and female HDs and *P. vivax*–infected patients, aged 18–60 yr, were recruited from the Amazon malaria-endemic area from the outpatient malaria clinic in the Tropical Medicine Research Center in Porto Velho, Brazil, with informed consent using a protocol approved by the Institutional Review Boards of the Oswaldo Cruz Foundation and National Ethical Council (CAAE: 59902816.7.0000.5091), University of Massachusetts Medical School (11116) and Boston Children's Hospital (00005698). The exclusion criteria were coinfection with *P. falciparum*, chronic inflammatory or infectious diseases, or pregnancy. Infected patients were clinically evaluated and tested for *Plasmodium* infection by thick smear and PCR during symptomatic stage and 40 days after treatment with chloroquine and primaquine. All relevant ethical regulations were followed while conducting this work.

Reagents. All antibodies and fluorescent dyes used in our experiments are listed in Supplementary Table S2.

Sample preparation. Peripheral blood mononuclear cells (PBMCs), obtained by Ficoll (GE Healthcare) gradient centrifugation as previously described[40], were stained for CD69, Ki67, HLA-DR, PFN, GNLY and GzmB. $CD8^+$ and $CD4^+$ T cells were purified from PBMCs by positive selection using Dynabeads (Thermo Fisher Scientific). The RBC pellet, suspended in isotonic Percoll, was used to purify iRetics from malaria patient samples on a 45% isotonic Percoll (GE Healthcare) gradient and uRetics from HDs on 70% Percoll. Uninfected erythrocytes (uRBCs) were obtained from the Percoll gradient pellet.

T lymphocyte and RBC coculture. Purified T cells (10^5/well) and Retics (5×10^5/well) were cocultured at 37 °C for 10 h in 96-well plates to assess T cell activation, IFN-γ production and degranulation (CD107a)[41]. Some experiments were performed in the presence of 2 µg/ml HLA-ABC blocking antibody (W6/33) or isotype control, which were added to $CD8^+$ T cells 30 min before RBC coculture. T lymphocytes cultured with 1 µg/ml anti-CD3 (BD Pharmingen) and 0.5 µg/ml anti-CD28 (BD Pharmingen) were used as positive controls.

Flow cytometry. T cell surface was stained with anti-CD4, anti-CD8, anti-CD3, anti-CD69, anti–HLA-DR, anti-Ki67, anti-CD19, anti-γδ TCR, anti-αβ TCR, anti-CD56, anti-CD161 and anti-TCRVα7.2. RBCs were stained with anti-CD71, anti-CD235a, anti–HLA-ABC (class I), anti–HLA-DR (class II), Thiazole Orange and SYBR Green I (*P. vivax* DNA)[25,42–44]. To analyze intracellular cytokine and granule protein expression, we incubated cells at 37 °C, 5% CO_2 in the presence of indicated stimuli for 30 min before adding brefeldin A (1 µl/ml) and monensin (1 µl/ml) (BD Pharmingen) solutions and culture for an additional 4–10 h before staining. Cells were first stained for indicated cell surface markers, then permeabilized in Fix/Perm buffer, and stained in Perm/Wash buffer (BD Pharmingen) for IFN-γ or cytotoxic granule proteins as per the manufacturer's instructions. Flow cytometry was performed using a FACScan flow cytometer (Becton Dickinson), Fortessa (Becton Dickinson) or Celesta (Becton Dickinson) and analyzed using FlowJo software V.10 (Tri-Star).

Plasma granulysin. GNLY in plasma from HDs and *P. vivax*–infected patients was measured using the Human Granulysin DuoSet ELISA (R&D Systems).

Reticulocyte protein expression. Cell lysates of iRetics and HD uRetics, obtained by lysis in radioimmunoprecipitation assay buffer (Sigma-Aldrich) in the presence of complete protease inhibitor (Roche), were analyzed by immunoblot probed for TAP1 after hemoglobin removal using HemogloBind (Biotech Support Group). Each retic lane was loaded with 50 µg of protein, whereas the PBMC control sample contained 20 µg of protein. The same membrane was probed for β-actin and F-actin as loading controls. β-Actin was used as loading control for HD uRetics and F-actin for iRetics because of host cell remodeling of the actin cytoskeleton under *Plasmodium* infection[45,46]. The secondary anti-mouse or anti-rabbit immunoglobulin-G antibody was detected by chemiluminescence.

Proteomic and transcriptomic analysis. Databases for the Retic proteome[23] and transcriptome[24] were analyzed for expression of proteins involved in the endogenous antigen presentation pathway (Supplementary Table S1) using ID_REF data deposited in the Gene Expression Omnibus (http://www.ncbi.nlm.nih.gov/geo/) (accession numbers: GSM143572–143599, GSM143671–143682, GSM143703, GSM143706–143716, GSM143718–143721).

Cytotoxic enzymes. GzmB, GNLY and PFN were purified from YT-Indy cells as described previously[47]. Purity was >95%, as determined by Coomassie-stained SDS-polyacrylamide gel electrophoresis. Protein concentrations were determined by Bradford assay. Specific activity of GNLY and PFN was determined by serial dilution on iRetics and uRetics; a sublytic concentration (<20% killing, adequate to deliver Gzms, but not kill most host cells) was used in all experiments. Specific activity of GzmB was determined by cleavage of the peptide substrate, *t*-Butyloxycarbonyl-Ala-Ala-Asp-ThioBenzyl ester, in the presence of 5,5′Dithio-bis (2-nitrobenzoic acid).

Reticulocyte lysis assay. iRetics labeled with CFSE (Sigma-Aldrich) were cultured with $CD8^+$ T cells at indicated ratios. Twelve hours later, cells were harvested and stained for CD235a and CD8. The number of surviving $CFSE^+$ gated $CD235a^+$ cells was compared with the number of $CFSE^+$ cells surviving after culture in the absence of lymphocytes. LDH release, measured by CytoTox 96 (Promega), was used to assess RBC lysis after coculture for 12 h with $CD8^+$ T cells at indicated Effector:Target (E:T) ratios. To assess cytolysis by purified granule proteins, we incubated iRetics for 1 h at 37 °C with 100 nM GNLY ± 500 nM GzmB ± a sublytic concentration of PFN and analyzed the culture supernatants by LDH release assay. The morphology of treated Retics was assessed by electron microscopy.

Parasite invasion assay. Invasion assays were performed as previously described[34]. iRetics from patients with *P. vivax* malaria, enriched on a 45% Percoll gradient, were treated with 100 nM GNLY ± 500 nM GzmB ± a sublytic concentration of PFN for 1 h at 37 °C. Uninfected HD reticulocytes, obtained from a 70% Percoll gradient, were added to the washed, treated iRetics at a ratio of 10:1. After 24-h coculture, cytospins were stained with Giemsa, and the proportion of newly invaded ring-stage-infected cells was enumerated.

Imaging flow cytometry. Purified $CD8^+$ T cells and Retics were cocultured at an E:T ratio of 1:5 for 1 h and then stained with HLA-ABC, TCR, CD3, CD8 and CD235a antibodies before analysis on an ImageStream Amnis X using Ideas software (Amnis). $CD235a^+CD3^+$ doublets were selected based on aspect ratio versus cell area. Purified iRetics and uRetics were incubated with 100 nM GNLY–AF488 or 500 nM GzmB–AF488 in the presence or absence of 100 nM unlabeled GNLY for 1 h at 37 °C as described previously[5]. Cells were washed and fixed with 2% paraformaldehyde in PBS before imaging flow cytometry. The frequency of cells staining for GNLY and GzmB was quantified using Ideas software. To analyze colocalization, we stained images of iRetics incubated for 1 h with 100 nM GNLY–AF647 and 500 nM GzmB–AF488 with CD235a-PE and Hoechst 33342.

Cholesterol depletion. HD RBCs in Hank's Balanced Salt Solution were untreated or incubated with indicated concentrations of methyl-β-cyclodextrin for 30 min at 37 °C before adding indicated amounts of purified GNLY and GzmB or GzmB–AF488 and culturing for 1 h. Treated cells were analyzed by flow cytometry for GNLY and GzmB uptake by flow cytometry or for LDH release as described earlier.

Electron microscopy. Purified iRetics incubated with 100 nM GNLY ± 500 nM GzmB were fixed in 2.5% buffered glutaraldehyde solution, 0.1 M (pH 7.2), for 3 h at 4 °C, washed, and the cell pellet was immersed in 4% agarose. The pellet was fixed in 1% osmium tetroxide and 1.5% (w/v) potassium ferrocyanide, dehydrated in ethanol, and embedded in Araldite 502 (Electron Microscopy Sciences). Extra-thin sections, obtained using a Sorvall MT-2B ultramicrotome (Dupont), were applied to 200-mesh copper grids (Ted Pella) and stained with 2% uranyl acetate and Reynolds' lead citrate. Images were obtained by transmission electron microscopy using a Tecnai G2-12 Spirit BioTWIN 120 kV (FEI).

Statistical analysis. Statistical analysis was performed using GraphPad Prism V7.0. Before applying statistical methods, whether the data fit a normal distribution was evaluated by the D'Agostino and Pearson normality test. The distribution was considered normal when $P \leq 0.05$. Parametric or nonparametric (Mann–Whitney test) two-tailed paired and unpaired *t*-tests were used to compare two groups at 95% confidence interval (CI). Multiple groups were compared by two-way analysis of variance (ANOVA) with additional Tukey's multiple comparisons test at 95% CI. Simple column comparisons were analyzed by one-way ANOVA using the Kruskal–Wallis test and Tukey's multiple comparisons test at 95% CI. Differences were considered statistically significant when $P \leq 0.05$. All of the *P* values less than 0.0001 are shown not as exact values but as $P < 0.0001$.

Reporting summary. Further information on experimental design is available in the Nature Research Reporting Summary linked to this article.

Data availability. The underlying data are available from the corresponding author on reasonable request.

References

40. Böyum, A. Isolation of mononuclear cells and granulocytes from human blood. Isolation of monuclear cells by one centrifugation, and of granulocytes by combining centrifugation and sedimentation at 1 g. *Scand. J. Clin. Lab. Invest. Suppl.* **97**, 77–89 (1968).
41. Betts, M. R. et al. Sensitive and viable identification of antigen-specific CD8+ T cells by a flow cytometric assay for degranulation. *J. Immunol. Methods* **281**, 65–78 (2003).
42. Cho, J. S. et al. Unambiguous determination of *Plasmodium vivax* reticulocyte invasion by flow cytometry. *Int. J. Parasitol.* **46**, 31–39 (2016).
43. Russell, B. et al. Field-based flow cytometry for ex vivo characterization of *Plasmodium vivax* and *P. falciparum* antimalarial sensitivity. *Antimicrob. Agents Chemother.* **57**, 5170–5174 (2013).

44. Wirjanata, G. et al. Quantification of *Plasmodium* ex vivo drug susceptibility by flow cytometry. *Malar. J.* **14**, 417 (2015).
45. Rug, M. et al. Export of virulence proteins by malaria-infected erythrocytes involves remodeling of host actin cytoskeleton. *Blood* **124**, 3459–3468 (2014).
46. Cyrklaff, M. et al. Hemoglobins S and C interfere with actin remodeling in *Plasmodium falciparum*-infected erythrocytes. *Science* **334**, 1283–1286 (2011).
47. Thiery, J., Walch, M., Jensen, D. K., Martinvalet, D. & Lieberman, J. Isolation of cytotoxic T cell and NK granules and purification of their effector proteins. *Curr. Protoc. Cell Biol.* **Chapter 3**, Unit 3.37 (2010).

nature research

Corresponding author(s): Ricardo T. Gazzinelli; Judy Lieberman; Caroline Junqueira

Life Sciences Reporting Summary

Nature Research wishes to improve the reproducibility of the work that we publish. This form is intended for publication with all accepted life science papers and provides structure for consistency and transparency in reporting. Every life science submission will use this form; some list items might not apply to an individual manuscript, but all fields must be completed for clarity.

For further information on the points included in this form, see Reporting Life Sciences Research. For further information on Nature Research policies, including our data availability policy, see Authors & Referees and the Editorial Policy Checklist.

Please do not complete any field with "not applicable" or n/a. Refer to the help text for what text to use if an item is not relevant to your study.
For final submission: please carefully check your responses for accuracy; you will not be able to make changes later.

Experimental design

1. Sample size

Describe how sample size was determined.

Our study was planned to enroll 30 individuals in each of our patient groups over the course of two years of the study. The hypothesis was that symptomatic malaria patients before treatment (SBT) should be different from symptomatic after treatment (SAT) and healthy donors (HD). Usually one would use a two sample t-test to make this comparison. In general, with n=30 in each group there is 80% power for a difference of 0.6 SD (shift of 0.6 standard deviations) or 90% power for shift of 0.7 SD. Indeed, were analyzed our published results from the same malaria endemic field and found that the differences observed in mean levels of (for example) cytokine or gene expression in the pre and post treatment symptomatic group of individuals with P. vivax was usually larger than this ৯C on the order of 1 SD difference. This power calculation suggests that given the expected sample size, we are robustly powered to achieve interpretable and meaningful results.
The sample size above was establish for ex vivo phenotypic analysis, presented in figures 1 and 2. For each ex vivo phenotypic characterization, the sample size had a minimum of 5 subjects in order to obtain a powerful significance. In addition, the assays were repeated with difference biological samples. The number of subjects was also dependent on the number of patients included in the study at each collection period.
The invitro assays in order to elucidate the immunological mechanisms were performed at least with n=4 per individually experiment, being n=3 the minimum required for 80% power. All the in vitro assays were also dependent in the number of subjects included at the collection period. For the Image cytometry analysis, a n=3 was used, since each sample collection generated 50.000 single cell data.

2. Data exclusions

Describe any data exclusions.

No data was excluded from our analysis.

3. Replication

Describe the measures taken to verify the reproducibility of the experimental findings.

All in vitro assays were performed at least twice with different subjects. The data presented is representative of one assay.
All attempts at replication were successfull.

4. Randomization

Describe how samples/organisms/participants were allocated into experimental groups.

The inclusion of participants in our study was completely randomized. Subjects were allocated as they arrived at the Research Center.

5. Blinding

Describe whether the investigators were blinded to group allocation during data collection and/or analysis.

All the imaging cytometry acquisition were performed blinded, in order to avoid any tendency to set the fluorescence background.

Note: all in vivo studies must report how sample size was determined and whether blinding and randomization were used.

6. Statistical parameters

For all figures and tables that use statistical methods, confirm that the following items are present in relevant figure legends (or in the Methods section if additional space is needed).

n/a	Confirmed
☐	☒ The exact sample size (*n*) for each experimental group/condition, given as a discrete number and unit of measurement (animals, litters, cultures, etc.)
☐	☒ A description of how samples were collected, noting whether measurements were taken from distinct samples or whether the same sample was measured repeatedly
☐	☒ A statement indicating how many times each experiment was replicated
☐	☒ The statistical test(s) used and whether they are one- or two-sided *Only common tests should be described solely by name; describe more complex techniques in the Methods section.*
☒	☐ A description of any assumptions or corrections, such as an adjustment for multiple comparisons
☐	☒ Test values indicating whether an effect is present *Provide confidence intervals or give results of significance tests (e.g. P values) as exact values whenever appropriate and with effect sizes noted.*
☐	☒ A clear description of statistics including central tendency (e.g. median, mean) and variation (e.g. standard deviation, interquartile range)
☐	☒ Clearly defined error bars in all relevant figure captions (with explicit mention of central tendency and variation)

See the web collection on statistics for biologists for further resources and guidance.

Software

Policy information about availability of computer code

7. Software

Describe the software used to analyze the data in this study.

Graphs design and statistical analysis was performed using GraphPad Prism V7.0. Proteomic and transcriptomic analysis were confronted to protein Blast and nucleotide Blast respectively. Image flow cytometry data were analysed by IDEAS Software from Millipore. Flow cytometry data were analysed by the Software FlowJo v. 10.4.2.

For manuscripts utilizing custom algorithms or software that are central to the paper but not yet described in the published literature, software must be made available to editors and reviewers upon request. We strongly encourage code deposition in a community repository (e.g. GitHub). *Nature Methods* guidance for providing algorithms and software for publication provides further information on this topic.

Materials and reagents

Policy information about availability of materials

8. Materials availability

Indicate whether there are restrictions on availability of unique materials or if these materials are only available for distribution by a third party.

The purified cytolitic enzymes were provided by Sumit Sen Santara and Farokh Dotiwala from Judy Lieberman lab.

9. Antibodies

Describe the antibodies used and how they were validated for use in the system under study (i.e. assay and species).

Each antibody and dye was validated as manufacturer instruction, general 1:200 dilution for the antibodies, 1:1000 dilution for LIVE/DEAD and SYBR Green and undiluted for the Retic count regent. Then, the antibodyes and the SYBR Green were titrated in order to obtain the best concentration to employed in our painels. The species was chosen according to the target subject.

ANTIGEN CONJUGATE SPECIES REACTIVITY CLONE MANUFACTURER CATALOG LOT
CD107 PE-Cy7 mouse anti-human H4A3 BD Pharmingen 561348 B212671
CD161 APC mouse anti-human HP-3G10 BioLegend 339911 B200986
CD19 FITC mouse anti-human HIB19 BD Pharmingen 555412 74576
CD235a PerCP eFluor 710 mouse anti-human GA-R2 eBioscience 46-9987-42 E11402-432
CD235a eFluor450 mouse anti-human HIR2 eBioscience 48-9987-41 E19491-102
CD28 Purified mouse anti-human CD28.2 BD Pharmingen 555725 5267879
CD3 Purified mouse anti-human HIT3a BD Pharmingen 555336 5354962
CD3 PerCP-Cy5.5 mouse anti-human UCHT1 BioLegend 300430 B221391
CD3 FITC mouse anti-human UCHT1 ebiscience 110038-73 E031967
CD4 APC mouse anti-human OKT4 BioLegend 317416 B217365
CD4 APC mouse anti-human RPA-T4 Invitrogen 470049 4324428
CD56 Alexa Fluor 700 mouse anti-human B159 BD Pharmingen 557919 7031700
CD69 FITC mouse anti-human FN50 BD Pharmingen 557049 26296
CD71 PE mouse anti-human M-A712 BD Pharmingen 555537 3909
CD8 APC mouse anti-human HIT8a BD Pharmingen 300911 B227823
CD8 APC-Cy7 mouse anti-human RPA-T8 BD Pharmingen 557760 7061979
F actin Unconjugated mouse anti-human NH3 Abcan ab205 GR269913-11
Granulysin Alexa Fluor 488 mouse anti-human RB1 BD Pharmingen 558254 8026721
Granzyme B APC mouse anti-human GB11 Invitrogen GRB05 1908524
HLA-ABC APC mouse anti-human W6/32 eBioscience 17-9983-42 E14162-104
HLA-ABC Functional Grade mouse anti-human DX17 BD Pharmingen 560187 2223625
HLA-ABC Functional Grade mouse anti-human W6/32 BioLegend 311412 B148491
HLA-DR eFluor780 mouse anti-human LN3 eBioscience 47-9956-42 4297875
IFN-γ PE-Cy7 mouse anti-human 4S.B3 BD Pharmingen 557844 E07674-211
IgG (H + L) HRP goat anti-mouse Polyclonal Abcan 97023 GR298142-9
IgG HRP donkey anti-rabbit Polyclonal GE Healthcare NA9340V 46544019
Ki67 PE mouse anti-human 20Raj1 eBioscience 12-5699-42 4276172
Mouse IgG2a κ Functional Grade not applicable eBM2a BioLegend 400224 B166872
Perforin PE mouse anti-human dG9 eBioscience 12-9994-42 E1 4120-104
TAP1 Unconjugated mouse anti-human 148.3 Merck MABF125 2768859
TCR Vα7.2 Alexa Fluor 700 mouse anti-human 3C10 BioLegend 351727 B207688
TCR αβ FITC mouse anti-human WT31 BD 347773 73640
TCR γδ PE mouse anti-human UC7-13D5 BioLegend 107507 B212475
β actin Unconjugated rabbit anti-human Polyclonal Sigma A2066 095M4765V

DYE SPECIFICITY MANUFACTURER CATALOG LOT
BD Retic-Count/ Thiazole Orange RNA BD 349204 63916
LIVE/DEAD Fixable Aqua Dead Cell Stain Dead cells Invitrogen L34957 1799640
SYBR™ Green I DNA Invitrogen S7563 871283

10. Eukaryotic cell lines

a. State the source of each eukaryotic cell line used.

No eukaryotic cell lines were used in sections a-d

b. Describe the method of cell line authentication used.

N/A

c. Report whether the cell lines were tested for mycoplasma contamination.

N/A

d. If any of the cell lines used are listed in the database of commonly misidentified cell lines maintained by ICLAC, provide a scientific rationale for their use.

N/A

Animals and human research participants

Policy information about studies involving animals; when reporting animal research, follow the ARRIVE guidelines

11. Description of research animals

Provide all relevant details on animals and/or animal-derived materials used in the study.

No animals were used in the study.

Policy information about studies involving human research participants

12. Description of human research participants

Describe the covariate-relevant population characteristics of the human research participants.

Patients infected with P. vivax and healthy donors (control group) living at endemic area for malaria in Porto Velho, Rondonia, Brazil, were included in our study. Both male and felamle individuals ranging from 21 to 59 years old with positive smears (higher than 501 parasites/ mmˆ3) and PCR+ were invited to enroll in the study, and after obtaining consent, was collect 100 ml of blood. Inclusion criteria for acute malaria included documented pyrexia (T> 38 ° C) or frank chill history within 48 h before recruitment and two diagnostic tests (thick smear and PCR). Symptomatic and health donor individuals should not have had malaria therapy in the past 6 months. Individuals co-infected with both Pf and Pv, pregnant women, people receiving treatment with immunosuppressive drugs, and individuals with infectious or chronic inflammatory diseases were excluded. The project was developed in collaboration with the group of researchers and physicians from the Research Center for Tropical Medicine of Rondonia (CEPEM) and FIOCRUZ Rondonia, who were in charged to enroll patients into our study. The IRB protocols were approved at Oswaldo Cruz Foundation and National Ethical Council (CAAE: 59902816.7.0000.5091), University of Massachusetts Medical School (11116) and Boston Children Hospital (00005698).